International Journal of GEOMATE, Dec., 2024 Vol.27, Issue 124, pp.128-135
ISSN: 2186-2982 (P), 2186-2990 (O), Japan, DOI: https://doi.org/10.21660/2024.124.4697
Geotechnique, Construction Materials and Environment

ESTIMATING THE PUNCHING SHEAR CAPACITY OF VOIDED REINFORCED CONCRETE SLAB

Quoc Anh Vu[1] and *Viet Chinh Mai[2]

[1]Department of Steel and Timber Structures, Hanoi Architectural University, Vietnam
[1]Institute of Techniques for Special Engineering, Le Quy Don Technical University, Hanoi, Vietnam

*Corresponding Author, Received: 08 Aug. 2024, Revised: 20 Oct. 2024, Accepted: 25 Oct. 2024

ABSTRACT: The study investigates the punching shear capacity of voided reinforced concrete (RC) slabs, which are increasingly utilized in modern construction due to their reduced weight and enhanced structural efficiency. Voided slabs, incorporating spherical or cylindrical voids, aim to mitigate the disadvantages of conventional RC slabs while maintaining structural integrity. Finite element models are developed to simulate their behavior under vertical load, validated by the results of a prior experimental study. The proposed simulation model is subsequently subjected to extensive parametric studies. The deflection of the slab, the crack propagation, and the punching shear capacity are analyzed. The findings reveal that the spacing from the face of the column to the first row of voids significantly influences the punching shear resistance of flat slabs. Additionally, analysis results obtained from the simulation method and those from current codes (ACI and Eurocode) are also discussed in this article. The results provide insights and practical recommendations for the design of voided slabs, suggesting that the first row of voids should be positioned at a distance greater than 1.5D from the column faces.

Keywords: Voided slab, Punching shear capacity, ACI 318-14, EN 1992-1-1, CDP model

1. INTRODUCTION

Voided slabs are increasingly utilized in contemporary construction, particularly in large-span structures, due to their economic advantages and material efficiency [1]. These slabs incorporate spherical or cylindrical voids, which reduce the overall concrete volume while maintaining structural performance. Fig. 1 compares the economic and technical parameters of conventional and voided slabs, using data from VRO Construction Joint Stock Company [2, 3] with real projects in Vietnam. These projects encompass complex buildings, apartments, shopping centers, and offices and include 39-story buildings. The data indicate that voided slabs offer significant advantages in terms of material savings and construction costs.

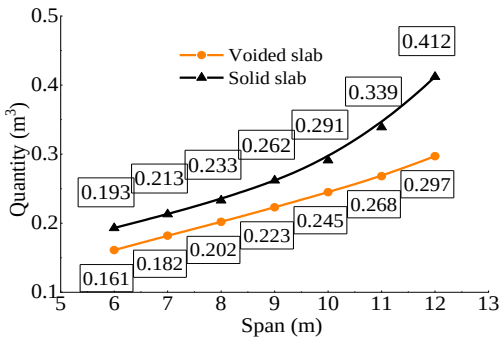

(a) Volume of concrete (m³) used per one m² of slab

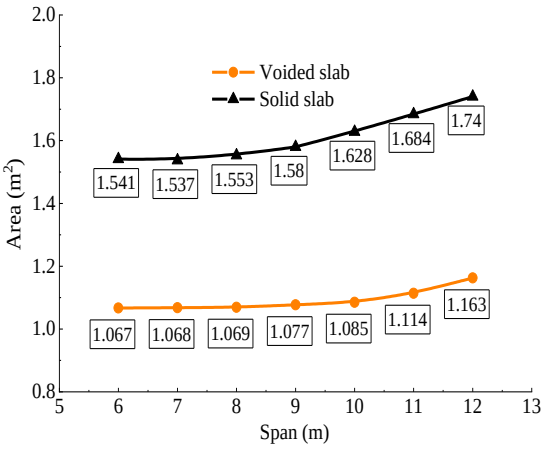

(b) Formwork cost per one m² of slab

Fig. 1 Comparison of technical and economic parameters of conventional and voided slabs [2, 3]

However, the introduction of voids complicates the evaluation of punching shear strength, a critical factor in ensuring the slab's capacity to withstand concentrated loads. In contrast to flexural failures, which often show warning signs through visible cracks and deflections, punching shear failures can occur abruptly without significant prior indications, thereby presenting significant safety risks [4]. This issue becomes even more serious with voided slabs.

Regarding the topic of punching shear capacity in voided slabs, several studies have been conducted, including notable ones. Most of these investigations adopt an experimental approach [5-8]. Nevertheless,

further research remains needed into the numerical simulation of punching shear resistance in voided slabs.

2. RESEARCH SIGNIFICANCE

Standards such as ACI and Eurocode do not include calculations related to voided slabs. Further studies on the punching shear resistance of voided slabs are necessary. Current research employs simulation methods to study the punching shear behavior of reinforced concrete voided slabs. The numerical model is validated through comparison with test results and subsequently developed to implement extensive parametric studies. Numerical simulation results are also compared with empirical formulas from current codes, and significant recommendations are provided for engineers when designing voided slab structures.

3. SIMULATION MODEL

3.1 Geometric Modelling

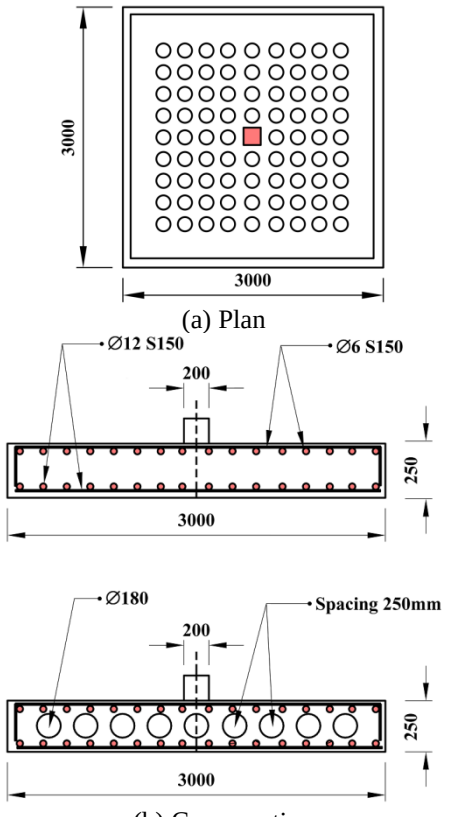

Fig. 2 Typical details of voided slabs

Full-scale simulation models are developed, including solid slabs and models incorporating spherical voids. The analysis of the solid slab aims to compare the punching shear capacity of voided and non-voided slabs. The spherical voids in the slab are positioned at various distances from the column face, with each void having a diameter of 180 mm. The arrangement and spacing of these voids are based on parameters from previous experimental studies [6, 8-10]. The slab has a plan dimension of 3000 mm × 3000 mm and a thickness of 250 mm. Steel reinforcing bars of 12 mm diameter are positioned at the bottom of the slab, while the top surface features bars with a diameter of 6 mm. The technical specifications of the simulation model, including plan dimensions, cross-sectional details, and reinforcements, are depicted in Fig. 2.

3.2 Material Parameters And Simulation Model Build-Up

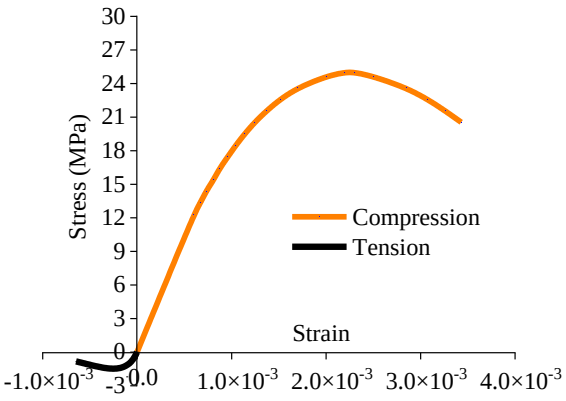

Fig. 3 Stress-strain curve of normal concrete [11]

Concrete used in the simulation possesses a compressive strength f_c = 25 MPa and elastic modulus E = 29780 MPa. The steel reinforcement bars possess the yielding strength f_y = 421 MPa, and Young's modulus of $E_s = 200\times10^3$ MPa. Fig. 3 illustrates the stress-strain curves of the concrete utilized in the simulation [11]. Concrete is known as a brittle, heterogeneous material that exhibits complex, nonlinear, inelastic behavior under multiaxial stress. To accurately capture these behaviors, selecting an appropriate model for simulating concrete is crucial. The Concrete Damaged plastic model (CDP model) is considered one of the most suitable models for this purpose. Initially proposed by Lubliner [12], the CDP model accounts for two primary damage mechanisms in concrete: tensile and compressive cracking. The evolution of the yield surface is governed by the material's hardening characteristics.

Abaqus is a comprehensive software suite used for simulating the behavior of materials and structures under various conditions [13-15]. In ABAQUS, CDP model is implemented using several parameters: the ratio between the biaxial compressive strength and the uniaxial compressive strength (σ_{bo}/σ_{co}), the failure parameter (kc), the

dilation angle (f), the eccentricity (ϵ), the viscosity parameter, and the material's stress-strain curve. These parameters are detailed in Table 1 [16, 17].

Table 1. Input parameters of CDP model for concrete in Abaqus [16, 17]

Parameter	σ_{bo}/σ_{co}	k_c	ϕ	ϵ	Viscosity
Value	1.16	2/3	31^0	0.1	0

The simulation model is developed using C3D8R elements for concrete and T3D2 elements for steel [18]. These elements have proven effective for simulating reinforced concrete structures [19-20]. Boundary conditions that prevent vertical displacement are applied to the slab's perimeter.

4. RESULTS AND DISCUSSION

4.1 Simulation Model Validation

To ensure the reliability of the analytical results, the simulation model must be verified against published experimental findings. Teng et al. (2018) [21] performed tests to determine the punching shear strength of solid slabs made from High Strength Concrete (HSC) that possess a compressive strength greater than 112 MPa. The slab has dimensions of 2.2 m × 2.2 m × 0.15 m. Vertical reinforcements of 16 mm diameter are arranged horizontally and vertically within the slab with a spacing of 118 mm.

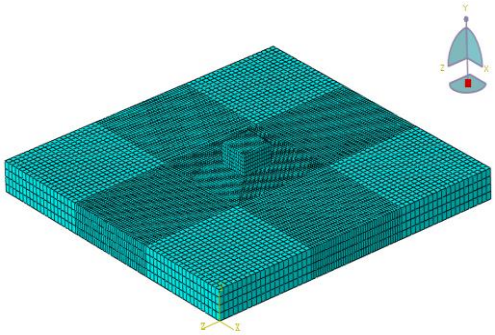

Fig. 4 3D simulation mesh model

To optimize the analysis time, the model is finely meshed with a size of 15 mm at a distance of 1/3 span from the center of the slab. In other regions, the mesh size is 25 mm. The 3D simulation model of the flat slab is subjected to a vertical load and mesh shape, as shown in Fig. 4.

The load-deflection curve at the middle span of slabs in accordance with the test [21] and the proposed numerical model is shown in Fig. 5. The simulation model determines the maximum capacity for punching shear of 489.6 kN at a deflection of 10.9 mm, whereas the experimental outcome reveal 454 kN corresponding to deflection of 10.3 mm. Comparison of the maximum values of punching shear according to the experiment and simulation model indicates a 7.8 % discrepancy.

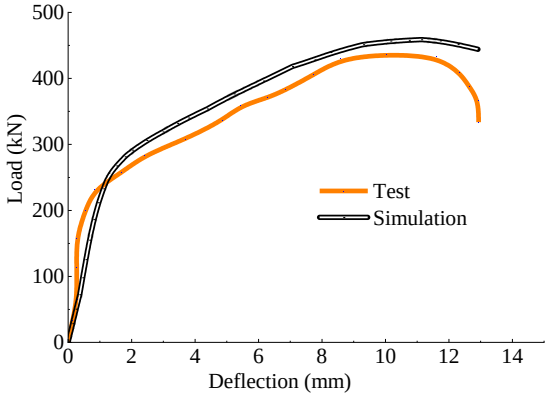

Fig. 5 Load-deflection curve according to the simulation and test of Teng [21]

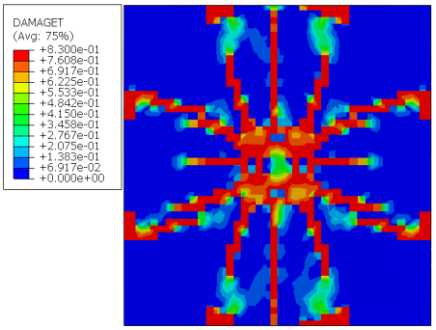

(a) Simulation

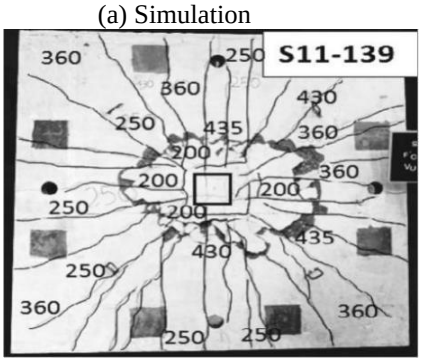

(b) Test

Fig. 6 Crack propagation observed in the simulation (a) and the test by Teng (b)

As observed in both the testing and simulation, Fig. 6 exhibits the crack propagation resulting from punching shear. Cracks form around the intersection between the floor slab and columns, spreading to the corners. These results demonstrate a good agreement between the test and simulation outcomes, affirming the reliability of the simulation model for further research.

4.2 Parametric Study

Extensive parametric studies were used for numerical simulation analysis, encompassing five cases, as shown in Table 2 and Fig. 7. The first case involves studying a solid flat slab under the punching shear. Cases 2 to 5 pertain to voided slabs, where the spacing from the face of the column to the first row of voids (S) is progressively reduced from 2D to 0.5D. Here, D = 225 mm represents the effective height of the slab having a thickness of 250 mm. The simulation model of voided slabs is shown in Fig. 8.

Table 2. Case study and results of simulation analysis

Case study	1	2	3	4	5
Type of slab	Solid slab	Voided slab	Voided slab	Voided slab	Voided slab
S	//	2D (450)	1.5D (337)	1D (225)	0.5D (113)
P (KN)	687.9	665.1	651.6	551.5	464.4

Note: D=225mm defines effective heigh of the slab; S denotes spacing (S) from first row of voids (mm); P is maximum punching shear force (KN)

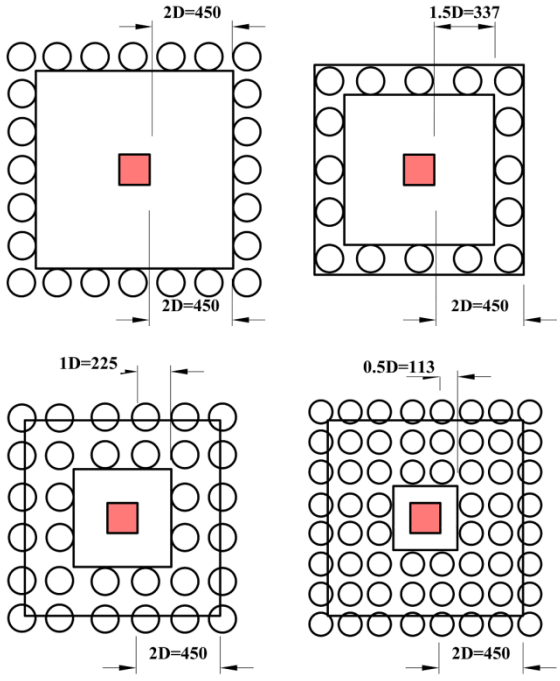

Fig. 7 Configurations of voided slabs with different spacing cases (S)

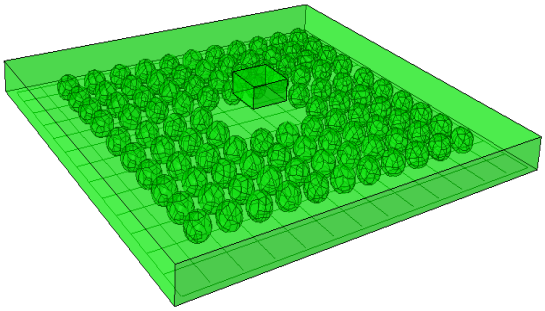

Fig. 8 Simulation model of voided slabs in Abaqus

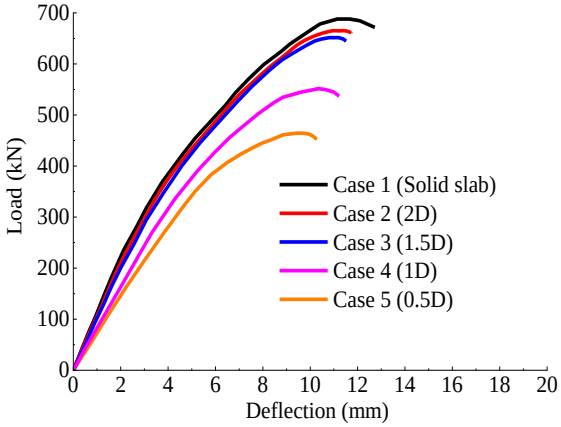

Fig. 9 Load-deflection curve from simulation

The load-deflection curves from numerical simulation, which exhibit a relatively similar shape and encompass three fundamental stages, are shown in Fig. 9. The first stage exhibits linear behavior, extending from the starting point to the point of crack formation. At the crack formation point, the punching shear force value is approximately one-third of the maximum value. The second stage, from the onset of crack formation to the peak of the curve, corresponds to nonlinear behavior. The third stage is characterized by a downward trend in the curve, where multiple cracks appear, leading to structural damage. In comparison to the curves of normal flexural structures, the curves of punching shear members lack a distinct yield plateau. The yield plateau is the stage where the load remains constant while the deformation of the structure continues to increase. This result aligns with the sudden failure characteristic of the structure under punching force, as recorded in previous experimental studies [8, 9]. Additionally, the load-deflection curves indicate that as the spacing between the column face and the first row of voids (S) decreases, the shear resistance capacity of voided slabs also decreases. The curves for cases 4 and 5 exhibit a substantially smaller slope compared to the remaining curves, indicating a notable decrease in stiffness. This can be attributed

to the increased number of voids in the critical area as S decreases, leading to a reduction in the loading capacity of the structure. When the distance from the edge of the column to the first void increases to 1.5D (case 3), the punching shear resistance of the voided slabs closely resembles that of the solid slabs, with only a 5% difference compared to case 1. However, when the spacing S decreases below 1.5D, the punching shear strength of slabs with voids largely diminishes. For instance, the punching shear capacity of case 3 (1.5D) is 18% and 40% greater than that of case 4 (1D) and case 5 (0.5D), respectively.

Fig. 10 depicts the crack formation in the voided slab. It can be observed that cracks initiate and propagate towards the corners of the slab. From the column edge, punching shear critical cones are formed that extend down to the tensile surface of the slab. Consequently, it is evident that the further the voids are from these punching shear cones, the less impact they have on the slab's loading capacity.

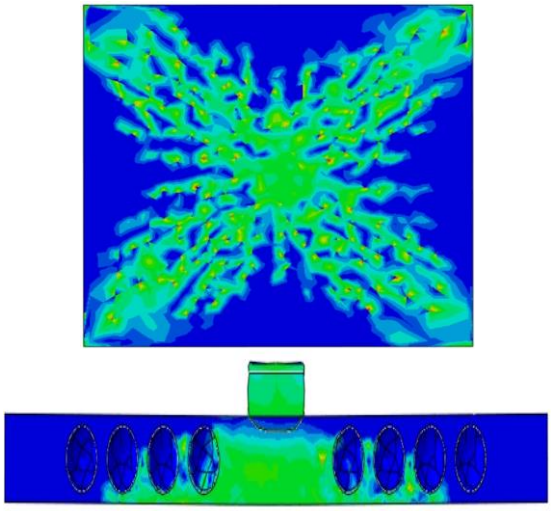

Fig. 10 Crack formation in voided slabs

4.3 Predicting The Punching Shear Capacity Of Slabs With Voids According To Various Code

Two widely applied codes for determining the punching shear strength of flat plates are ACI 318-2014 [22] and Eurocode 1992-1-1 [23]. The shear capacity according to these codes is determined by three main parameters: the critical section, the shear strength of the concrete, and the effect of flexural reinforcing bars.

The punching shear capacity of solid plates (V_c) in ACI 318-2014 is determined as the minimum value calculated using the following equations:

$$V_c = 0.33\lambda\sqrt{f_c}.A \quad (1)$$

$$V_c = 0.17(1+2/\beta)\lambda\sqrt{f_c}A \quad (2)$$

$$V_c = 0.083(2+\alpha_s D/b_0)\lambda\sqrt{f_c}A \quad (3)$$

Where: λ is a coefficient equivalent to 1 for conventional concrete;

f_c is the compressive strength of cylindrical concrete specimen; b_0 defines the perimeter value for the critical shear section of the slab;

D denotes the effective value of the slab's depth

β represents the ratio between the height and width of the column. The constant αs has a value of 40 specifically for the inner column; $A = b_o \times D$ represents the concrete area. The value of b_0 is illustrated in Fig. 11.

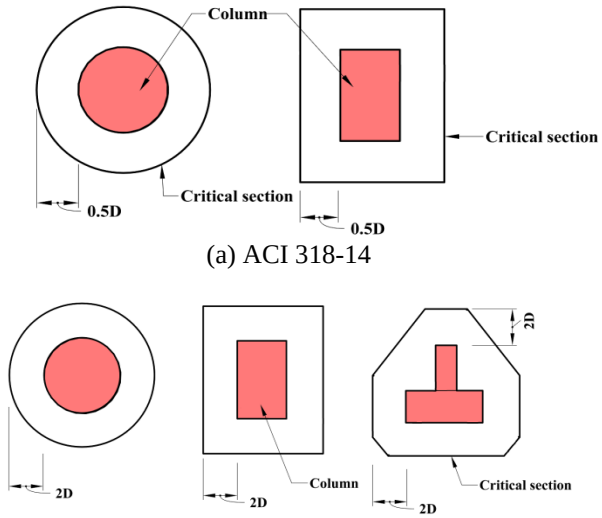

Fig. 11 Determination of critical section according to ACI 318-14 and EN 1992-1-1

EN 1992-1-1, in contrast with ACI 318-14, states that the critical section for punching shear is located at a position of 2d beyond the face of the column. The punching shear of a slab $V_{Rd,c}$ can be obtained by the following equations:

$$V_{Rd,c} = C_{Rd,c}k(100\rho f_c)^{1/3}A \quad (4)$$

$$k = 1+\sqrt{200/D} \le 2 \quad (5)$$

$C_{Rd,c}$ is equal to 0.18; k is the size effect coefficient, calculated according to Eq. 5; ρ represents the ratio of longitudinal reinforcement in the slab.

From the above formulas, it can be observed that the punching shear capacity of slabs in ACI 318-14 and EN 1992-1-1 applies only to solid structures. The influence of voids needs to be considered. Sagadevan [8] proposed a formula to calculate the effective area of a voided slab according to the equation:

$$A_e = b_i D - A_{i(void)} \quad (6)$$

The control perimeter, b_i, is dependent upon the position of the void, while A_i(void) represents the void area at the i_{th} critical part (i = 0, 1,…n), as shown in Fig. 7. It is necessary to calculate the smallest value of A_e.

Tables 3-7 compare the highest possible punching shear capacity as per the ACI 318-14, EN 1992-1-1, and simulation for distances S from the column face to the first row of void, corresponding to different cases detailed in Table 2. It should be noted that the ACI 318-14 code considers only a critical cross-section of 0.5D, whereas the EN 1992-1-1 considers 2D. Consequently, cases where the spacing S exceeds 0.5d will be calculated solely according to the EN 1992-1-1.

Table 3 Punching shear capacity with solid slab (case 1)

D	A_e	V_c ACI	V_c EN	(ACI+EN)	Sim.	Dis.
(mm)	(mm^2)	(kN)	(kN)	(kN)	(kN)	(%)
225	382500	631.1	668.8	649.9	687.9	5.8

Note: ACI+EN is the average value; Sim.: Simulation; Dis.: Disparity

Table 4 Punching shear capacity with voided slab (case 2)

D	A_e	V_c ACI	V_c EN	(ACI+EN)	Sim.	Disparity
(mm)	(mm^2)	(kN)	(kN)	(kN)	(kN)	(%)
225	382500	//	668.8	668.8	665.1	0.6

Table 5 Punching shear capacity with voided slab (case 3)

D	A_e	V_c ACI	V_c EN	(ACI+EN)	Sim.	Dis.
(mm)	(mm^2)	(kN)	(kN))	(kN)	(kN)	(%)
225	317700	//	555.1	555.1	651.6	17.4

Table 6 Punching shear capacity with voided slab (case 4)

D	A_e	V_c ACI	V_c EN	(ACI+EN)	Sim.	Dis.
(mm)	(mm^2)	(kN)	(kN)	(kN)	(kN)	(%)
225	252900	//	442.2	442.2	551.5	24.7

Table 7 Punching shear capacity with voided slab (case 5)

D	A_e	V_c ACI	V_c EN	(ACI+EN)	Sim.	Dis.
(mm)	(mm^2)	(kN)	(kN)	(kN)	(kN)	(%)
225	237600	392.0	415.4	403.7	464.4	15

All cases of predicting the punching shear capacity according to ACI 318-14 and EN 1992-1-1 codes show conservative and smaller results compared to the simulation. For solid slabs, the disparity between the punching shear capacity from simulation and the codes is relatively small (5.8%). When the distance S is greater than 2D, this difference is small. However, for distances S smaller than 2D, the difference between simulation and formulas proposed by codes ranges from 15% to 24.7%. This considerable discrepancy is because the codes do not accurately represent the actual performance of voided slabs.

Table 8 presents a comparison of the punching shear forces of voided slabs based on some experimental tests and calculations according to the formulas in ACI 318-14 and EN 1992-1-1. The calculations in ACI and Eurocode consider the reduced area created by voids in the slab, as described in Equation 6. It is observed that in most cases, when the distance from the column surface to the first hollow row (S) is greater than 1.5D, the difference between the code-based calculations and the experimental results is less than 12%. However, when this distance (S) is reduced to 0.5D, the difference between the experimental values and the code-based calculations increases to up to 33%.

5. CONCLUSION

The current work adopts the simulation approach to investigate the punching shear capability of RC voided slabs. The findings obtained lead to the following conclusions:

When the distance S from the column edge to the first void, is greater than 1.5D (where D denotes the effective thickness of the voided slab), the punching shear resistance is almost equivalent to that of a solid slab. However, when S is reduced below 1.5D, the punching shear capacity of the voided slab significantly decreases.

In all analysed cases, the punching shear capacity calculated according to the ACI 318-14 and EN 1992-1-1 is conservative and smaller than the simulation results. When S is greater than 1.5D, the punching shear force calculated by ACI and Eurocode shows a negligible difference compared to the simulation. However, with S less than 1.5D, the

Table 8 Comparison of punching shear capacity according to tests and calculations by ACI 318-14, EN 1992-1-1

Ref.	ID	Void location from column face	Effective depth D, (mm)	Test, (kN)	Maximum load			
					Available codes			
					ACI 318	Test / ACI 318	EN 1992	Test / EN 1992
Sagadevan et al. (2019) [8]	V1	<1.5D	135	239.8	//	//	210.1	1.14
	V2	<D/2	135	240.4	194.6	1.24	200.5	1.20
	V3	<D/2	135	574.4	460.3	1.25	476.5	1.21
	V4	<1.5D	225	548.9	//	//	488.7	1.12
	V5	>2D	225	657.2	//	//	614.7	1.07
	V6	>2D	225	672.3	//	//	614.7	1.09
	V7	>2D	225	653.6	//	//	614.7	1.06
Oukaili and Husain (2017) [24]	BD1	2D	77	140	//	//	128.8	1.09
	BD3	2D	105	205	//	//	190.5	1.08
	BD5	d	77	120	//	//	101.7	1.18
	BD7	d	105	190	//	//	157.4	1.21
	BD9	2D	77	180	//	//	162.3	1.11
	BD11	2D	105	325	//	//	303.1	1.07
	BD13	d	77	170	//	//	141.6	1.20
	BD15	d	105	290	//	//	235.8	1.23
Valivonis et al. (2017a) [25]	BPR1-1	<D/2	234	600.1	485.3	1.24	501.8	1.20
	BPR1-2	<D/2	234	600.2	485.3	1.24	501.8	1.20
	BPR2-1	<D/2	234	776.3	584.1	1.33	600.8	1.29
	BPR2-2	<D/2	234	704.4	584.1	1.21	600.8	1.17
	BPR3-1	>D	150	385.4	//	//	400.7	0.96
	BPR3-2	>D	150	428.1	//	//	400.7	1.07
Chung et al. (2018a) [26]	PD-N-0	1.5D	215	758.1	//	//	700.2	1.08
	PD-N-4	<D/2	215	677.1	545.9	1.24	563.3	1.20
	PD-N-8	<D/2	215	641.5	523.7	1.22	542.2	1.18
Han and Lee (2014) [27]	V1	>D/2	380	1297	//	//	1087.5	1.19
	V2	<D/2	373	1071	857.4	1.25	890.3	1.20
	V3	<D/2	373	1111	875.3	1.27	898.1	1.24
	V4	<D/2	373	944	760.6	1.24	784.8	1.20

difference between simulation results and codes increases to 24.7%. Current standards do not, in fact, include calculations regarding the punching shear strength of voided slabs. Based on the obtained results, the authors recommend that, in the design of voided slabs, the first row of voids should be placed at a distance greater than 1.5D from the face of the columns.

6. REFERENCES

[1] Al-Azzawi, A.A., and Mtashar, S.H., Behavior of two-way reinforced concrete voided slabs enhanced by steel fibers and GFRP sheets under repeated loading. Results in Engineering, Vol. 17, 2023, pp.100872.

[2] Projects. 2024 [cited 2024; Available from: https://vro.vn/projects/].

[3] S-VRO Foam core floor. Viet Nam: VRO Construction Jointstock Company, 2024.

[4] Isufi, B., Ramos, A.P., and Lúcio, V., Post-earthquake performance of a slab-column connection with punching shear reinforcement. Journal of Earthquake Engineering, Vol. 26, Issue 3, 2022, pp.1171-1193.

[5] Abbas, A.N., and Jaafer, E.K., Punching Shear Behavior of Voided Reinforced Concrete Flat Plate Panels. International Journal of

Engineering Research Technology, 2018, pp.0974-3154.
[6] Azizian, H., Lotfollahi-Yaghin, M.A., and Behravesh, A., Punching Shear Strength of Voided Slabs on the Elastic Bases. Iranian Journal of Science Technology, Transactions of Civil Engineering, Vol. 45, 2021, pp.2437-2449
[7] Kanth, L.L., and Poluraju, P., Structural Behaviour of Voided Flat Slab with Various Void Ratios Under Vertical Loading. Civil and Environmental Engineering, Vol. 19, Issue 1, 2023, pp.301-317.
[8] Sagadevan, R., and Rao, B., Experimental and analytical investigation of punching shear capacity of biaxial voided slabs. Structures, Vol. 20, 2019, pp.340–352.
[9] Khouzani, M.A., Zeynalian, M., Hashemi, M., Mostofinejad, D., and Farahbod, F., Study on shear behavior and capacity of biaxial ellipsoidal voided slabs. Structures: Elsevier, 2020, pp. 1075-1085.
[10] Said, M., Mahmoud, A.A., and Salah, A. Performance of reinforced concrete slabs under punching loads. Materials and Structures, Vol. 53, Issue 4, 2020, pp.68.
[11] Ding, Y., and NING, X., Mechanical Behavior of Materials. Reinforced Concrete: Basic Theory and Standards, Singapore: Springer Nature Singapore, 2023, pp.9-57.
[12] Lubliner, J., Oliver, J., Oller, S., Oñate, E., and structures., A plastic-damage model for concrete. International Journal of solids, Vol. 25, Issue 3 1989, pp.299-326.
[13] Akhmad, R.H.P., Influence of seawater on strength of concrete beams strengthened with glass fiber reinforced polymer sheet. International Journal of GEOMATE, Vol. 26, Issue 117, 2024, pp.35-42.
[14] Khassaf, S.I., Chkheiwr, A., and Jasim, M.A., Effect of contraction joints on the structural performance of arch dam. International Journal of GEOMATE, Vol. 19, 2020, pp.219-227.
[15] Olarewaju, A.J., Estimation of blast loads for studying the dynamic effects of coeffcient of friction on buried pipes by simulation. International Journal of GEOMATE, Vol. 7, Issue 13, 2014, pp.1017-1024.
[16] Hafezolghorani, M., Hejazi, F., Vaghei, R., Jaafar, M.S.B., and Karimzade, K., Simplified damage plasticity model for concrete. Vol. 27, Issue 1, 2017, pp.68-78.
[17] Systèmes, D. Abaqus/CAE User's Guide, 2016.
Alsabhan, A.H., Sadique, M.R., Ahmad, S., Alam, S., and Binyahya, A.S., The effect of opening shapes on the stability of underground tunnels: A finite element analysis. International Journal of GEOMATE, Vol. 21, Issue 87, 2021, pp.19-27
[18] Huang, F., Wang, T., and Lin, Y., Evaluation of Fastener Flexibility in Hybrid CFRP and Metal Joints Using the Finite Element Method. Journal of Physics: Conference Series: IOP Publishing, 2023, pp.012010.
[19] Sahu, O., Das, P., Choudhury, S., Pradhan, N., Basa, B., and Jena, B., On transverse crack effects in beams under free vibration using finite element analysis. Materials Today: Proceedings, 2024.
[20] Zang, X., Wang, G., Zhang, Z., Duan, X., and Hu, X., Study on Mechanical Behavior of Reinforced Concrete Beams under Sulfate Attack. Advances in Civil Engineering, Vol. 1, 2022, pp.3465281.
[21] Teng, S., Chanthabouala, K., Lim, D.T.Y., and Hidayat, R., Punching shear strength of slabs and influence of low reinforcement ratio. ACI Structural Journal, 2018, pp.139-150.
[22] ACI Committee 318: Building Code Requirements for Structural Concrete (ACI 318-14) and Commentary (ACI 318R-14). American Concrete Institute: Farmington Hills, MI, 2014.
[23] Eurocode 2: Design of concrete structures - Part 1-1: General rules and rules for buildings. The European Union, 2004.
[24] Oukaili, N.K., and Husain, L.F., Punching shear in reinforced concrete bubbled slabs: experimental investigation. Smart monitoring, assessment rehabilitation of civil structures, Zurich, Switzerland, 2017.
[25] Valivonis, J., Šneideris, A., Šalna, R., Popov, V., Daugevicius, M., and Jonaitis, B., Punching strength of biaxial voided slabs. ACI Structural Journal, Vol. 114, Issue 6, 2017, pp.1373-1383.
[26] Chung, J.-H., Bae, B.-I., Choi, H.-K., Jung, H.-S., and Choi, C.-S., Evaluation of punching shear strength of voided slabs considering the effect of the ratio b0/d. Engineering Structures, Vol. 164 , 2018, pp.70-81.
[27] Han, S.W., and Lee, C.S., Evaluation of punching shear strength of voided transfer slabs. Magazine of concrete research, Vol. 66, Issue 21 2014, pp.1116-1128.